ISSN 2070-0482, Mathematical Models and Computer Simulations, 2019, Vol. 11, No. 1, pp. 97–106. © Pleiades Publishing, Ltd., 2019.
Russian Text © V.V. Vyshinsky, G.B. Sizykh, 2018, published in Matematicheskoe Modelirovanie, 2018, Vol. 30, No. 6, pp. 21–18.

The Verification of the Calculation of Stationary Subsonic Flows and the Presentation of Results

V. V. Vyshinsky[a, b, *] and G. B. Sizykh[a, **]

[a] *Moscow Institute of Physics and Technology, Moscow, 141701 Russia*
[b] *Central Aerohydrodynamic Institute, Zhukovsky, Moscow oblast, 140180 Russia*
**e-mail: vyshinsky@rambler.ru*
***e-mail: o1o2o3@yandex.ru*

Received April 19, 2017

Abstract—The principle of pressure maximum is proved for a stationary three-dimensional vortex ideal gas flow (without the assumption of barotropicity). Based on the fact that in regions where the solution is modeled with a high degree of accuracy within the boundary value problem for the Euler equations, the consequences of the Euler equations must also hold, and the obtained subsonic principle is proposed to be used for verification of the numerical solutions of the boundary value problems for Euler equations for an ideal gas and for the Navier-Stokes equations for viscous gas. The conditions of the maximum principle include the value of the Q-parameter, whose surface level image is currently widely used to visualize the flow pattern. The proposed principle of the maximum pressure reveals the meaning of the surface $Q = 0$. It divides the flow region into the subdomain $Q > 0$ in which there can be no local pressure maximum and subdomain $Q < 0$ in which there can be no local pressure minimum. A similar meaning of parameter Q was known for incompressible fluid (H. Rowland, 1880; G. Hamel, 1936). The expression for the Q-parameter contains only the first derivatives of the velocity components, which allows determining the sign (+/–) of Q even for numerical solutions obtained by the low-order methods. An example of the numerical solution's verification using the subsonic principle of the pressure maximum is presented. Analysis of the results of the numerical calculation of the flow around a moving aircraft carrier in the presence of atmospheric winds showed that if the calculation results are used for the simulation of complex flight modes and analyze the state of the atmosphere from the point of view of safe air traffic, visualizing the flow pattern by $Q = \text{const}$ surfaces is not informative. In particular, these surfaces do not reflect the true picture of the wind shear perceived by the aircraft directly entering it. To verify the numerical method, it is sufficient to provide only a surface $Q = 0$ which has a clear physical meaning.

Keywords: Euler equations, Navier-Stokes equations, subsonic vortex flows, subsonic principle of pressure maximum, correctness of problems, forms of presenting calculation results, verification of calculation results

DOI: 10.1134/S2070048219010162

INTRODUCTION

When solving atmospheric problems, it is necessary to take into account the mass forces $\mathbf{F} = \rho\mathbf{g}$. The corresponding system of Euler equations can be written as

$$\frac{\partial}{\partial t}\begin{Vmatrix}\rho\\ \rho\mathbf{V}\\ \rho E\end{Vmatrix} + \nabla\begin{Vmatrix}\rho\mathbf{V}\\ \rho\mathbf{V}^2\\ (\rho E + p)\mathbf{V}\end{Vmatrix} = \begin{Vmatrix}0\\ -\nabla p + \rho\mathbf{g}\\ \rho\mathbf{g}\cdot\mathbf{V}\end{Vmatrix}, \tag{1}$$

where ρ is the density, p is the pressure, $\mathbf{V}$ is the velocity, and ρE is the total energy of a unit of volume (the dot between the vectors stands for the scalar product). The first equation expresses the condition of mass conservation; the following three, the conservation of momentum; and the energy equation completes the system.

Equations (1) adequately describe the transfer of vorticity and have three physical mechanisms for its generation: entropy, energy (in accordance with the Crocco theorem for a steady flow $\mathbf{V}\times\mathrm{rot}\mathbf{V} = -T\cdot\nabla S + \nabla H_0$, where T is the temperature, S is the enthropy, and H_0 is the total enthalpy), and density

(in accordance with the Bjerknes theorem, the pressure field can create circulation in the case where $\rho \neq$ const on the $p =$ const surface).

In any numerical scheme, instead of the original system (1), the following system of equations is solved

$$\frac{\partial}{\partial t}\begin{Vmatrix}\rho\\ \rho\vec{V}\\ \rho E\end{Vmatrix} + \nabla\begin{Vmatrix}\rho\mathbf{V}\\ \rho\mathbf{V}^2\\ (\rho E + p)\mathbf{V}\end{Vmatrix} = \begin{Vmatrix}0\\ -\nabla(p\bar{\bar{\mathbf{I}}} + \bar{\bar{\mathbf{W}}}) + \rho\mathbf{g}\\ -\bar{\bar{\mathbf{W}}} : \nabla\mathbf{V} + \rho\mathbf{g}\mathbf{V}\end{Vmatrix},$$

where $\bar{\bar{\mathbf{I}}}$ is the unit tensor and $\bar{\bar{\mathbf{W}}}$ is the tensor of circuit and/or artificial viscosity. In other words, both diffusion and dissipative terms are present in the numerical scheme, although the processes they model do not reflect reality, since the system of equations (1) does not have viscous terms. In the absence of real viscous diffusion on the difference grid, it is impossible to describe waves whose length is shorter than the grid step. In a numerical experiment, the problems of the adequacy of the grid density and the sufficiency of the order of approximation of the numerical scheme, the computational domain size, and/or the possibility of applying nonreflecting boundary conditions are solved. At the same time, the question of the accuracy of the solutions obtained for nonlinear systems remains open, since the convergence of the numerical solution to the solution of the original boundary value problem is proved only for the linear case (the Lax theorem). Therefore, despite the existence of the well-known verification methods, any additional way of checking the adequacy of numerical simulation results is of value.

In the most complex flows, there are zones in which a simpler boundary value problem can be solved, for example, laminar sections in a turbulent flow, zones of stationarity and potentiality of the flow, and flow regions where viscosity and compressibility can be neglected.

If there are zones in the flow field that are modeled with a high degree of accuracy within the boundary value problem for the Euler equations, then the consequences of the Euler equations must also hold in them. In this paper we suggest checking the fulfillment of one of these consequences for the additional verification of the numerical calculations in the boundary value problems for the Euler and Navier-Stokes equations. This is about the subsonic principle of the pressure maximum, previously unknown and first proposed in this article.

The first theorems on the extremal values of the pressure following from the fluid motion equations include the following three theorems. The Rowland theorem [1] is for an ideal incompressible fluid, the Poincaré theorem [2] is for an incompressible fluid in a gravitational field created by the fluid itself, and the Hamel theorem [3] is for a viscous incompressible fluid (it can be found in the monograph [4, §28] by Serrin). These theorems state that the pressure cannot reach a minimum or a maximum at an internal point of the flow. In the process of proving these theorems, harmonic and subharmonic equations for the pressure were obtained and then the versions of the principle of maximum valid for such equations were used. Statements were obtained about the minimum or maximum, depending on the sign of parameter Q, the expression for which only includes the first spatial derivatives of the velocity component (this expression will be presented later). The expression does not contain second derivatives, which is convenient for verifying numerical solutions, because that reduces the requirements for the order of accuracy and for the grid's fineness when determining the sign of parameter Q.

In [5] the principles of the pressure maximum were obtained for the $\int dp/\rho$ value in the barotropic gas flows. However, their conditions depend on the values calculated from the second derivatives of the velocity components. In comparison with the conditions of the Hamel theorem [3] (for an incompressible fluid), these values contain an additional term, $\partial I/\partial t + \mathbf{V}\cdot\nabla I$, where $I = \mathrm{div}\mathbf{V}$. The presence of this term complicates the verification of numerical solutions for checking the fulfillment of the theorem [5], since even in the stationary case the expression $\partial I/\partial t + \mathbf{V}\cdot\nabla I$ contains second spatial derivatives of the velocity components. Moreover, in [5] the theorems are proven only for barotropic gas, which substantially narrows the flow types under consideration.

In this paper the principle of the pressure maximum is obtained for subsonic stationary ideal gas vortex flows. The conditions of this maximum principle include only the parameter Q (or more precisely, only its sign). The flow can be nonbarotropic. This means that the entropy function, while remaining constant along the streamline, can be different on different streamlines. The resulting maximum principle differs from the subsonic maximum principle obtained by Schiffman in [6] (the formulation and proof can be found in [7, ch. II]). The difference is that the Schiffman principle refers not to pressure but to velocity,

and it is proved only for barotropic and vortex-free flows, while the principle of the pressure maximum obtained in this article can also be used to verify the calculations for vortex gas flows.

THE PRINCIPLE OF THE PRESSURE MAXIMUM FOR SUBSONIC STATIONARY IDEAL GAS FLOWS

We consider a stationary subsonic ideal gas flow in a certain closed region $\bar{G}$. Using the notation of the previous section, the fluid's motion is described by Euler equations written in the form [2, 8]

$$\mathbf{\Omega}\times\mathbf{V} = -\frac{1}{\rho}\nabla p - \frac{1}{2}\nabla V^2 + \mathbf{g}, \quad V = |\mathbf{V}|, \quad \mathbf{\Omega} = \mathbf{rot}\,\mathbf{V}, \tag{2}$$

$$\mathrm{div}(\rho\mathbf{V}) = 0. \tag{3}$$

The pressure p and the density ρ are related by the expression $p = \sigma\rho^k$, where k is the adiabatic index and σ is the enthropy function. It can be different on different streamlines but remains constant along each specific streamline:

$$\mathbf{V}\cdot\nabla(\rho^{-k}p) = 0. \tag{4}$$

The flow is assumed to be subsonic; i.e., the velocity value V at each point of the closed region $\bar{G}$ is assumed to be lower than the local sound velocity $\sqrt{kp/\rho}$:

$$\mathrm{M} = V/\sqrt{kp/\rho} < 1. \tag{5}$$

In the studied closed region $\bar{G}$ all the hydrodynamic parameters are assumed to be twice continuously differentiable functions of the coordinates.

If we take the divergence of both sides of Eq. (2) and use the known identity for the divergence of the vector product $\mathrm{div}(\mathbf{c}\times\mathbf{d}) \equiv \mathbf{d}\cdot\mathbf{rot}\,\mathbf{c} - \mathbf{c}\cdot\mathbf{rot}\,\mathbf{d}$, we get the equation

$$\mathbf{V}\cdot\mathbf{rot}\,\mathbf{\Omega} - \Omega^2 = -\frac{1}{\rho}\Delta p + \frac{1}{\rho^2}\nabla p\cdot\nabla\rho - \frac{1}{2}\Delta V^2, \tag{6}$$

where Δ is the Laplace operator. If we denote the velocity $\mathbf{V}$ components in an arbitrary rectangular Cartesian coordinate system *Oxyz* by *u*, *v*, *and w*, then direct verification shows the validity of the equality

$$0.5\Delta V^2 = \mathbf{V}\cdot\Delta\mathbf{V} + (\nabla u)^2 + (\nabla v)^2 + (\nabla w)^2, \tag{7}$$

where, for example, $(\nabla u)^2$ means the squared gradient of u, the velocity component. Because of another known vector identity $\nabla\mathrm{div}\,\mathbf{c} \equiv \mathbf{rot}\,\mathbf{rot}\,\mathbf{c} + \Delta\mathbf{c}$, the first term of the left part of (6) is written as

$$\mathbf{V}\cdot\mathbf{rot}\,\mathbf{\Omega} = \mathbf{V}\cdot\nabla\mathrm{div}\mathbf{V} - \mathbf{V}\cdot\nabla\mathbf{V}. \tag{8}$$

Equations (7) and (8) allow us to eliminate the velocity Laplacian $\Delta\mathbf{V}$ from Eq. (6). After permutation of the terms, we obtain the equation

$$\frac{1}{\rho}\Delta p + \mathbf{V}\cdot\nabla\mathrm{div}\mathbf{V} - \frac{1}{\rho^2}\nabla p\cdot\nabla\rho = 2Q, \tag{9}$$

where

$$Q = 0.5(\Omega^2 - (\nabla u)^2 - (\nabla v)^2 - (\nabla w)^2). \tag{10}$$

Note. Parameter Q can be written as $Q = 0.5(\overline{\overline{\Omega}}_{ij}\overline{\overline{\Omega}}_{ij} - \overline{\overline{S}}_{ij}\overline{\overline{S}}_{ij})$, where $\overline{\overline{\Omega}}_{ij} = 0.5(\partial u_i/\partial x_j - \partial u_j/\partial x_i)$ is the antisymmetric vorticity tensor and $\overline{\overline{S}}_{ij} = 0.5(\partial u_i/\partial x_j + \partial u_j/\partial x_i)$ is the symmetric strain rate tensor.

Then the expression for the second term of the left part of (9) is transformed. For this Eqs. (3) and (4) are presented in an equivalent form: $\mathrm{div}\mathbf{V} = -\mathbf{V}\cdot\nabla\ln\rho$ and $\mathbf{V}\cdot\nabla\ln p = k\mathbf{V}\cdot\nabla\ln\rho$. From these equations it follows that

$$\mathbf{V}\cdot\nabla\mathrm{div}\mathbf{V} = -\frac{1}{k}\mathbf{V}\cdot\nabla(\mathbf{V}\cdot\nabla\ln p). \tag{11}$$

The gradient of the scalar product included in the right part of (11) can be rewritten using two identities of the vector analysis: $\nabla(\mathbf{a}\cdot\mathbf{b}) \equiv (\mathbf{a}\cdot\nabla)\mathbf{b} + (\mathbf{b}\cdot\nabla)\mathbf{a} + \mathbf{a}\times\mathbf{rot}\,\mathbf{b} + \mathbf{b}\times\mathbf{rot}\,\mathbf{a}$ and $(\mathbf{a}\cdot\nabla)(\gamma\mathbf{b}) \equiv \gamma(a\cdot\nabla)\mathbf{b} + ((a\cdot\nabla)\gamma)\mathbf{b}$, where γ is the scalar function. As a result, taking into account the identity $\mathbf{rot}\,\nabla\ln p \equiv 0$, we get the equality

$$\mathbf{V}\cdot\nabla\mathrm{div}\mathbf{V} = -\frac{1}{kp}\mathbf{V}\cdot((\mathbf{V}\cdot\nabla)\nabla p) + \frac{1}{kp^2}(\mathbf{V}\cdot\nabla p)^2 - \frac{1}{kp}\mathbf{V}\cdot((\nabla p\cdot\nabla)\mathbf{V}) - \frac{1}{kp}\mathbf{V}\cdot(\nabla p\times\mathbf{rot}\,\mathbf{V}).$$

Therefore (9) takes the form

$$\begin{aligned}&\frac{1}{\rho}\Delta p - \frac{1}{kp}\mathbf{V}\cdot((\mathbf{V}\cdot\nabla)\nabla p) + \left\{\frac{1}{kp^2}(\mathbf{V}\cdot\nabla p)^2\right.\\ &\left. - \frac{1}{kp}\mathbf{V}\cdot((\nabla p\cdot\nabla)\mathbf{V}) - \frac{1}{kp}\mathbf{V}\cdot(\nabla p\times\mathbf{rot}\,\mathbf{V}) - \frac{1}{\rho^2}\nabla p\cdot\nabla\rho\right\} = 2Q.\end{aligned} \tag{12}$$

If we write Eq. (12) in the coordinate form and group the factors for the first and second derivatives of pressure, we obtain the equation

$$a_{11}\frac{\partial^2 p}{\partial x^2} + 2a_{12}\frac{\partial^2 p}{\partial x\partial y} + a_{22}\frac{\partial^2 p}{\partial y^2} + 2a_{13}\frac{\partial^2 p}{\partial x\partial z} + 2a_{23}\frac{\partial^2 p}{\partial y\partial z} + a_{33}\frac{\partial^2 p}{\partial z^2} + b_1\frac{\partial p}{\partial x} + b_2\frac{\partial p}{\partial y} + b_3\frac{\partial p}{\partial z} = 2Q, \tag{13}$$

where coefficients a_{11}, a_{12}, a_{22}, a_{13}, a_{23}, a_{33}, b_1, b_2, and b_3 depend on hydrodynamic parameters (u, v, w, p, ρ) and on their first derivatives. The expression inside curly brackets in (12) corresponds to the last three terms of the left part of (13).

If Eq. (13) is used to find the solution of the Euler equations from which it follows, the coefficients of the pressure derivatives cannot be regarded as known functions of the coordinates. However, if Eq. (13) is used to determine the properties of its solution under the assumption that such a solution exists, then these coefficients can be regarded as certain known functions of the coordinates. This approach was repeatedly used in the proofs, for example, in [6, 7, 9–12]. Equation (13) is considered from this point of view; i.e., the coefficients of the p derivatives in the left part of (13) and the right part of Q are assumed to be specified functions of the coordinates x, y, z. As mentioned above, when Eq. (12) is written in the coordinate form (13), the coefficients of the left part of Eq. (13) are expressed through the hydrodynamic parameters and their first derivatives. Taking into account the assumption that the second derivatives of the hydrodynamic parameters are continuous in $\bar{G}$, and also the fact that the density and pressure in the stationary subsonic flow cannot become zero, then a direct verification can confirm the following properties of the coefficients of Eq. (13).

A1. All the a_{11}, a_{12}, a_{22}, a_{13}, a_{23}, a_{33}, b_1, b_2, and b_3 coefficients and Q are continuous (and bounded) in $\bar{G}$.

A2. Using the Sylvester criterion and taking into account (5) shows that the coefficients of the second derivatives of p in Eq. (13), that is, a_{11}, a_{12}, a_{22}, a_{13}, a_{23}, and a_{33} are coefficients of a positive definite quadratic form.

A3. The determinant of the matrix A, composed of the coefficients a_{11}, a_{12}, a_{22}, a_{13}, a_{23}, and a_{33}, is equal to $\det A = \rho^{-3}(1 - \mathrm{M}^2)$. By condition (5) and the continuity of the gas-dynamical parameters in the closed flow region $\bar{G}$, there exists a number $\delta > 0$ such that at each point of $\bar{G}$ the condition $\det A > \delta$ holds.

Note that for these three properties to be valid, it would be sufficient to assume that the first derivatives of the hydrodynamic parameters are continuous. A stronger condition, the continuity of the second derivatives, is required in this study to validate the vector analysis formulas used in deriving Eq. (13).

The A1–A3 properties of the coefficients of Eq. (13) make it possible to apply to this equation two versions of the Hopf theorem [13, 14], depending on the sign of Q. These variants are formulated in [15] specifically for the three-dimensional case, when the coefficients of the equation are functions of three variables x, y, and z and are defined in some three-dimensional region G.

First, in [15] the following general assumption is formulated for the coefficients of the equation (in [15] this assumption is under number 3.1).

Assumption 1. Suppose that at all points of G the coefficients a_{11}, a_{12}, a_{22}, a_{13}, a_{23}, and a_{33} in the equation

$$a_{11}\frac{\partial^2 u}{\partial x^2} + 2a_{12}\frac{\partial^2 u}{\partial x\partial y} + a_{22}\frac{\partial^2 u}{\partial y^2} + 2a_{13}\frac{\partial^2 u}{\partial x\partial z} + 2a_{23}\frac{\partial^2 u}{\partial y\partial z} + a_{33}\frac{\partial^2 u}{\partial z^2} + b_1\frac{\partial u}{\partial x} + b_2\frac{\partial u}{\partial y} + b_3\frac{\partial u}{\partial z} + cu = f \tag{14}$$

are coefficients of the positive definite quadratic form A. Suppose that for each point $M(x, y, z) \in G$ such $\omega = \omega(x, y, z) > 0$ and $\Delta = \Delta(x, y, z) > 0$ exist that a closed ball $\bar{U}(M; \omega)$ lies entirely within G and in it all the coefficients of Eq. (14) are bounded and inequality $\det A > \Delta$ is fulfilled.

Then in [15] a series of statements is given depending on the properties of the coefficients of Eq. (14). In particular, in [15] these statements are under numbers 3.6 and 3.7.

Statement 1. Suppose that $c = 0$, $f \le 0$ in a bounded region G and Assumption 1 holds. If the solution $u \in C^2(G)$ of Eq. (14) is continuous in the closed region $\bar{G}$, then $u \ge \min_{\partial G} u$ in the entire G region. In this case, if $u \ne \text{const}$ in G, the equality $u = \min_{\partial G} u$ only holds in ∂G.

Statement 2. Suppose that $c = 0$, $f \ge 0$ in a bounded region G and Assumption 1 holds. If the solution $u \in C^2(G)$ of Eq. (14) is continuous in the closed region $\bar{G}$, then $u \le \max_{\partial G} u$ in the entire G region. In this case, if $u \ne \text{const}$ in G, the equality $u \le \max_{\partial G} u$ only holds in ∂G.

Comparing Eqs. (13) and (14) and the A1–A3 properties of the coefficients of Eq. (13) allows us to apply the variants given above of the Hopf theorem to Eq. (13) for the cases $Q < 0$ and $Q > 0$. Since $Q \ne 0$, the case of $p \equiv \text{const}$ is not possible and extremes are reached only at the boundary. Eventually we obtain the following main result.

Subsonic principle of the pressure maximum. Suppose that all hydrodynamic parameters are twice continuously differentiable functions of coordinates in a certain bounded closed region $\bar{G}$ of a stationary ideal gas flow. Suppose also that in $\bar{G}$ Eqs. (2)–(4) and inequality (5) are fulfilled and Q is defined by formula (10). Then, if at all points of $\bar{G}$ inequality (1) $Q < 0$ holds, then the pressure cannot have a local minimum at an internal point $\bar{G}$; and if at all points of $\bar{G}$ inequality (2) $Q > 0$ holds, then the pressure cannot have a local maximum at an internal point of $\bar{G}$.

Note that in both cases it is impossible to reach not only strict extrema but also nonstrict extrema at the interior point of $\bar{G}$.

USING THE PRINCIPLE OF THE PRESSURE MAXIMUM FOR VERIFICATION OF THE NUMERICAL METHODS

As is the case when using the Rowland, Poincaré, and Hamel theorems, Eq. (10), containing only the first derivatives of the velocity components, makes it possible to determine the sign of Q even for numerical solutions obtained by low-order methods. In this case, the existence of a local pressure minimum or maximum in a certain flow region is determined by a simple iteration over the values at the computational grid nodes. Therefore, the verification of the fulfillment of the maximum principle formulated above can be used as a verification method for a wide class of numerical calculations of fluid flows (both viscous and ideal).

If we arbitrarily divide the gas flow region into small zones, then in many of these zones (namely, in those far from the sources of vorticity), the flow can be vortical; however, the gas can be considered inviscid and its motion can be described by the Euler equations. Therefore, in such zones the maximum principle can be used to verify calculations even if these calculations were made for a viscous gas.

As an example, we consider the results of the numerical simulation in the boundary value problem for Reynolds-averaged Navier–Stokes equations (RANS) of a flow around a moving tactical aircraft carrier (TACC) in the presence of atmospheric wind [16].

The part of the ship that is above the waterline, from the aerodynamics point of view, is an elongated blunt body with vortical separation zones fixed on the sharp edges of the hull and superstructures. This ensures the Reynolds self-similarity of the flow and makes it possible to use the wind tunnel model tests for validation of the calculated flow parameters over the flight decks and in the vortex wake behind the part of the ship that is above the water.

An anisotropic model of turbulence in the surface layer was used as the atmosphere background. In the coordinate system associated with the ship the free-stream velocity profile has a potential component caused by the movement of the ship and the atmospheric wind component related to the no-slip condition on the sea surface. A random impulse is imposed on the averaged field [17]. A boundary value problem is solved for stationary Reynolds-averaged Navier-Stokes equations in the case of an incompressible fluid flow (the bar denotes Reynolds averaging):

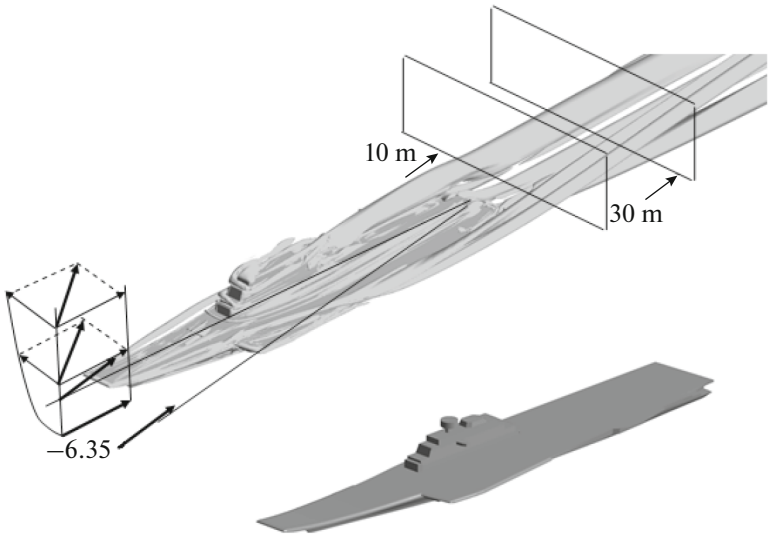

Fig. 1. Problem setup. Vortex structures are visualized by $Q = 0$ surfaces.

$$\rho\frac{\partial \overline{u}_j\overline{u}_i}{\partial x_j} = \rho\overline{f}_i + \frac{\partial}{\partial x_i}\left[-\overline{p}\delta_{ij} + \mu\left(\frac{\partial \overline{u}_i}{\partial x_j} + \frac{\partial \overline{u}_j}{\partial x_i}\right) - \rho\overline{u_i'u_j'}\right],$$

where $\rho\frac{\partial \overline{u}_j\overline{u}_i}{\partial x_j}$ is the change of the gas momentum; $\rho\overline{f}_i$ characterizes the action of external forces; $\overline{p}\delta_{ij}$ are the pressure forces; $\mu\left(\frac{\partial \overline{u}_i}{\partial x_j} + \frac{\partial \overline{u}_j}{\partial x_i}\right)$ is the action of forces related to viscosity; and $\rho\overline{u_i'u_j'}$ are the turbulent stresses. The SST turbulence model, which is the synthesis of the k–ω model (used in the wall-adjacent areas) and k–ε model (for the free flow region far from solid surfaces), was chosen to close the system of equations.

A mathematical model of a TACC was constructed in which all fairly large structural elements are realized; the ship had a length of 285 m, a width of 55 m, and a height of 50 m. The model was implemented in the calculation domain with the following dimensions: 1200 × 300 × 150 m. The computational grid contained 46 million nodes. The calculation was performed for the angle of the apparent wind β (the angle between the velocity vector of the free stream and the longitudinal axis of the ship in the ship's system in the horizontal plane) of 6 degrees at deck level (Fig. 1). The ship's velocity was about 20 knots and the atmospheric side wind determined the indicated β value.

To verify the numerical method using the maximum principle proposed in this paper, we consider the trailing vortex region of 100 m (width) × 60 m (height) × 20 m (length in the longitudinal direction). Figure 1 presents the extreme sections ($x = -10$ m and $x = -30$ m) of the considered area. The grid spacing is 1 m in all directions. The initial section of the trail is located 10 m behind the edge of the ship's stern.

The simulation results are shown in Figs. 2–7. Isobars (Fig. 2a) and the wind shear field $\partial u/\partial y$ are presented in the first section of the solution's verification area $x = -10$ m (the wind shear restrictions are available in the flight manual for most aircraft) (Fig. 2b). The cross marks the local pressure minimum in this section (the 2-D minimum point). It makes sense to look for a local 3-D minimum, which is mentioned in the subsonic principle of the pressure maximum obtained above, only at such points. By numerical differentiation, the gradients of the velocity and pressure components were found, and the tensors of the vorticity and deformation rates, as well as their contraction Q (formula (10)), were formed. For the numerical differentiation, a second-order difference scheme was used everywhere, including the boundary nodes of the computational grid.

Figures 3 and 7 present components of the vorticity tensors and strain rates. The pressure gradient components for section $x = -30$ m are shown in Figs. 4 and 5. Figure 5 also shows the $Q =$ const level field in the same section. The dark crosses mark the position of the (two-dimensional) pressure maximum in

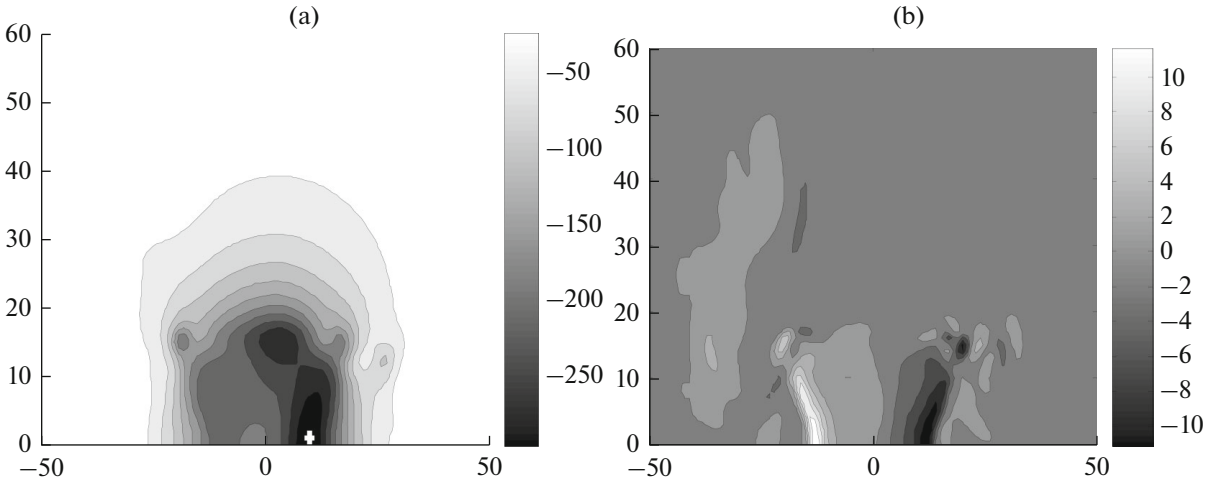

Fig. 2. Section $x = -10$ m: (a) isobars; (b) $\partial u/\partial y$.

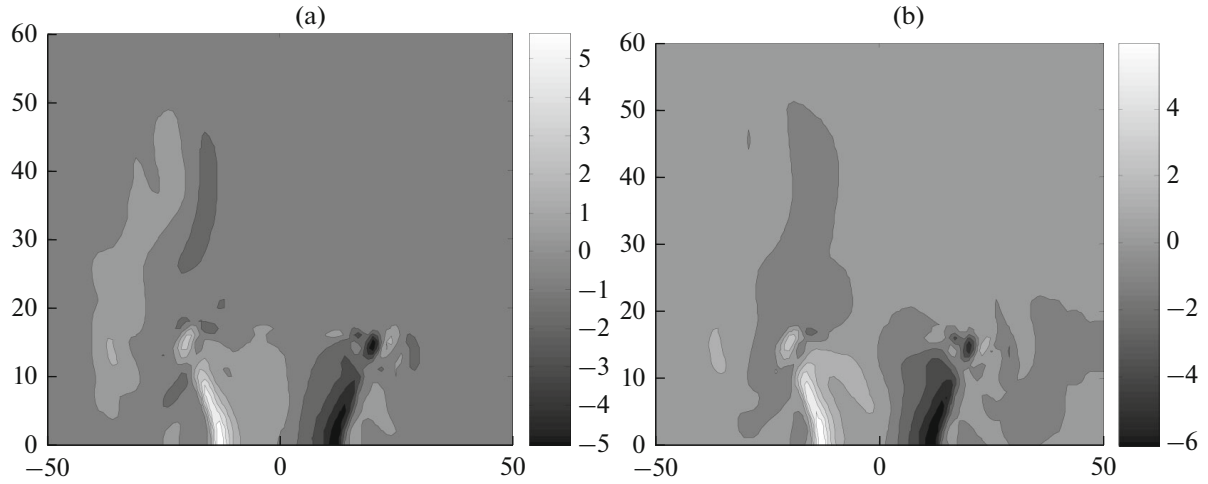

Fig. 3. Section $x = -10$ m: (a) $\overline{\overline{\Omega}}_{xy}$; (b) $\overline{\overline{S}}_{xy}$.

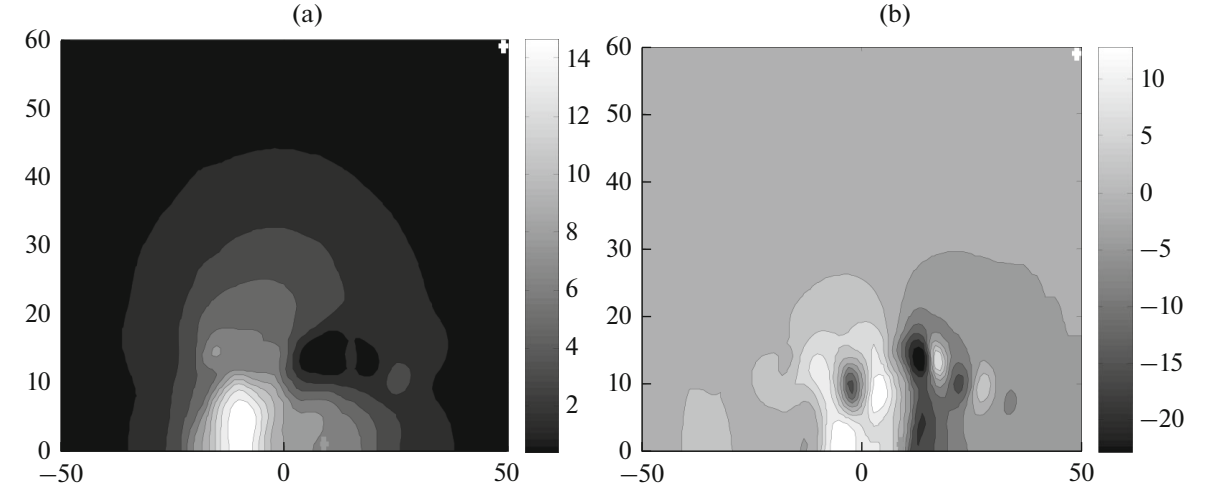

Fig. 4. Section $x = -30$ m: pressure gradient components (a) $\partial p/\partial x$; (b) $\partial p/\partial y$.

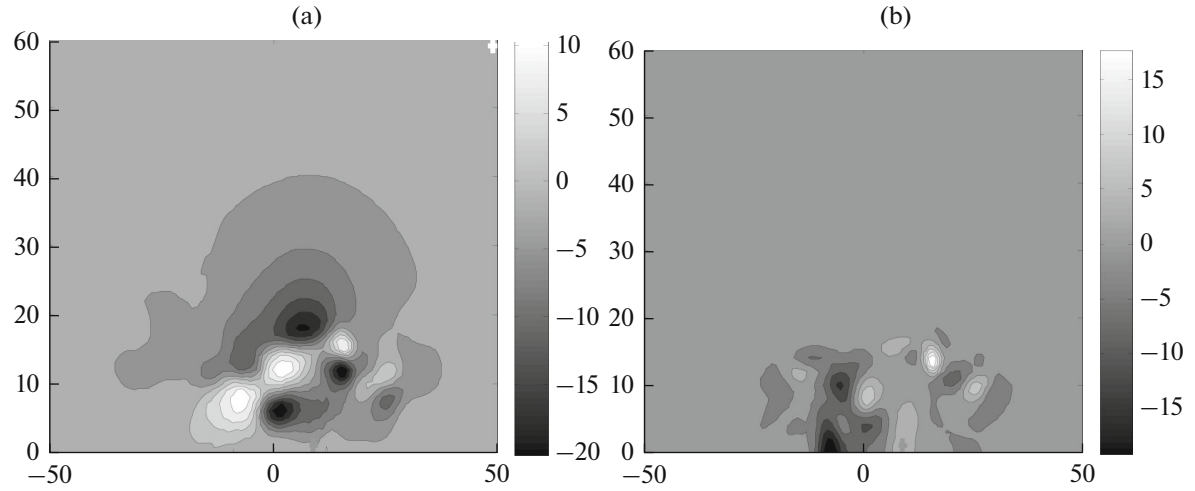

Fig. 5. Section $x = -30$ m: (a) pressure gradient components $\partial p/\partial z$; (b) Q = const levels.

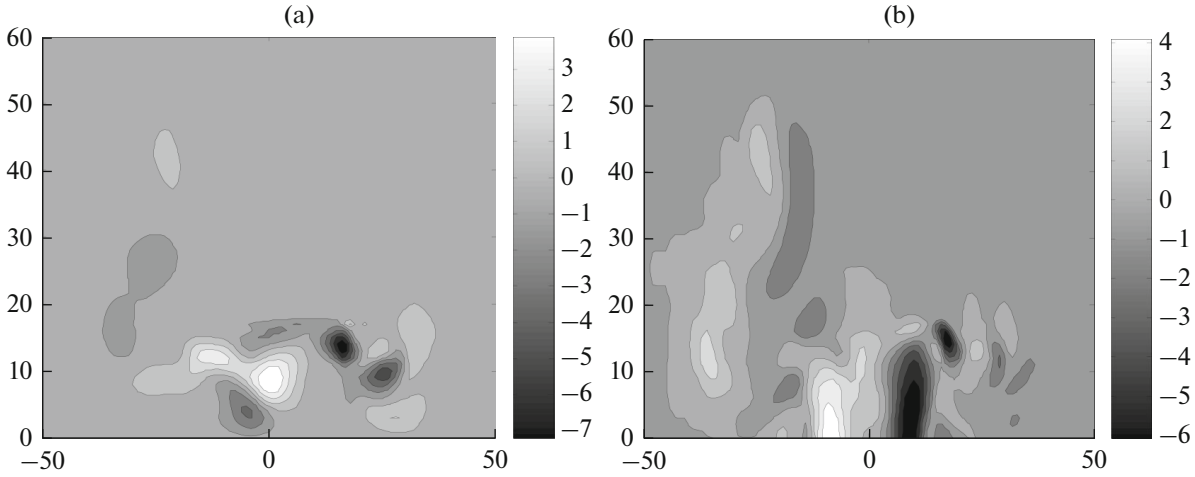

Fig. 6. Section $x = -30$ m: (a) Ω_x; (b) $\partial u/\partial y$.

this section. Figure 6 presents the longitudinal component of vorticity Ω_x and the $\partial u/\partial y$ levels for section $x = -30$ m.

The analysis of the calculation results using the subsonic principle of the pressure maximum obtained above did not reveal any contradictions. In particular, the studied section of the computational domain contains neither local 3-D pressure minima nor local 3-D maxima, which can serve as confirmation of the correctness of the implemented numerical scheme, the sufficiency of the numerical simulation domain size, fineness of the grid, order of approximation, the number of completed iterations and, indirectly, as confirmation of the boundary value problem correctness.

VISUALIZATION OF THE CALCULATION RESULTS

As stated in the introduction, Truesdell could not find such a condition for the principle of the pressure maximum (or rather, for the $\int dp/\rho$ value), which depends only on the first derivatives of the velocity components, even for a barotropic gas. (As shown in this paper, the sign of parameter Q turned out to be this condition for pressure.) However, it can be assumed that, possessing a highly scientific intuition, Truesdell sensed the importance of parameter Q for (compressible) gas flows. This is probably why in [5] he

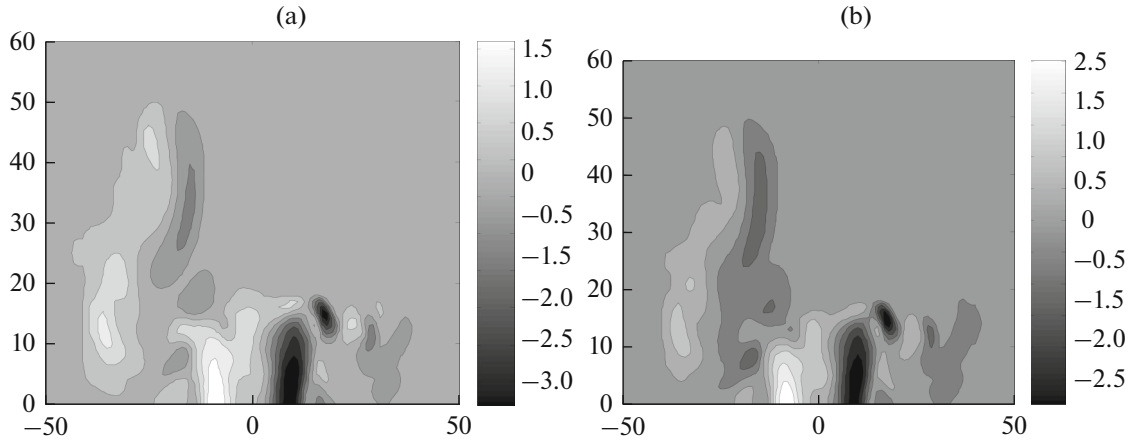

Fig. 7. Section $x = -30$ m: (a) $\overline{\overline{\Omega}}_{xy}$); (b) $\overline{\overline{S}}_{xy}$.

attempted to find the physical meaning of parameter Q and gave a number of convincing examples showing that in some cases Q represents the intuitive perception of vorticity by physicists and mechanics as the quantity characterizing that complexity of the fluid's motion that distinguishes it from the motion of a solid body better than the squared rotor Ω^2. In other cases, he considered Ω^2 to be the most adequate characteristic. As a result, he proposed a dimensionless quantity Ω^2/Q as a "second measure of vorticity." This proposal is still controversial and therefore is not included in textbooks on hydrodynamics.

However, one intermediate result of [5] turned out to have wide practical application. Some experimental physicists have found the physical meaning of parameter Q, discovered by Truesdell, to be most adequate for their concept of the flow's complexity [18, 19]. In [19] it was suggested to consider flow zones in which parameter Q is greater than a certain nonnegative threshold value as zones of rotating vortices of a turbulent flow (eddy-zones). Although there is no strict definition of the eddy- or E-zone, since then the image of Q-level parameter surfaces is used as one of the ways of visualizing E-zones of turbulent flows [19]. In many software systems, it is possible to represent the surfaces of the Q-parameter level and using such a representation of the calculation results is now considered the norm [20–23].

This paper clarifies the meaning of the $Q = 0$ surface. It divides the zones in which the pressure cannot reach either a minimum or a maximum (depending on the sign of Q). In order to clarify the meaning of $Q = \text{const} \neq 0$ surfaces, the calculation results for the atmospheric wind flow around the aircraft-carrying cruiser were used once again. The $Q = \text{const}$ surfaces with different constant values were compared to the velocity and pressure fields (these parameters are of key importance for aircraft). No connection was observed. These surfaces do not represent the true picture of the wind shear perceived by the aircraft directly entering it. In particular, the presence of a wake behind the "island" (ship superstructures) is reflected in the $\partial u/\partial y$ fields (Figs. 2b, 6c) and $\overline{\overline{\Omega}}_{xy}$ and $\overline{\overline{S}}_{xy}$ fields (Fig. 3). The Q field (Fig. 5b), however, does not represent the wake.

Therefore, it is proposed to apply a different visualization of the calculation results depending on their purpose. If the calculation is intended for comparison with the experimental data, which, as a rule [23], contain information about the surfaces of the level of parameter Q , then the representation of such surfaces will be useful for comparing the calculation with the experiment. If, however, the calculation results are to be used to simulate different flight modes, then the data on the surfaces of the level of the Q parameter are not very informative.

CONCLUSIONS

The popular [20–23] surfaces, which do not have a clear physical meaning of the surface $Q = \text{const} \neq 0$, do not reflect the true picture of the wind shear perceived by the aircraft directly entering it.

In accordance with the principle of the pressure maximum proposed in the article, only the $Q = 0$ levels separating the $Q > 0$ flow regions, in which there can be no local pressure maximum, from the $Q < 0$ regions, in which there can be no local pressure minimum, are meaningful. Therefore, to analyze a flow

in a wake, it is sufficient to construct only the $Q = 0$ surface. Moreover, the freed information space should be filled with the field images of other parameters important for aircraft. For example, to indicate the locations of the cores of the vortex which are quite clearly determined using the λ_2 criterion [19].

Along with the existing verification methods, it is proposed to use the subsonic principle of the pressure maximum proposed in this article as an additional accuracy criterion for stationary viscous gas flow calculations.

REFERENCES

1. H. Rowland, "On the motion of a perfect incompressible fluid when no bodies are present," Am. J. Math. **3**, 226–268 (1880).
2. H. Lamb, *Hydrodynamics* (Cambridge Univ. Press, Cambridge, 1895).
3. G. Hamel, "Ein allgemeiner Satz uber den Druck bei der Bewegung volumbestandiger Flussigkeiten," Monatsh. Math. Phys. **43**, 345–363 (1936).
4. J. Serrin, *Mathematical Principles of Classical Fluid Mechanics* (Springer, Berlin, Gottingen, Heidelberg, 1959).
5. C. Truesdell, "Two measures of vorticity," J. Rational Mech. Anal. **2**, 173–217 (1953).
6. M. Shiffman, "On the existence of subsonic flows of a compressible fluid," J. Rational Mech. Anal. **1**, 605–652 (1952).
7. L. Bers, *Mathematical Aspects of Subsonic and Transonic Gas Dynamics* (Wiley, New York, 1958).
8. L. G. Loytsyansky, *Mechanics of Liquids and Gases* (Pergamon, Oxford, 1966; Gostekhizdat, Moscow, 1950).
9. D. Gilbarg and M. Shiffman, "On bodies achieving extreme value of the critical Mach number. I," J. Ration. Mech. Anal. **3**, 209–230 (1954).
10. A. N. Burmistrov, V. P. Kovalev, and G. B. Sizykh, "Maximum principle for solving an equation of elliptic type with unbounded coefficients," Tr. MFTI **6** (4), 97–102 (2014).
11. G. B. Sizykh, "A sign of the presence of a deceleration point in a plane irrotational perfect gas flow," TRUDY MFTI **7** (2), 108–112 (2015).
12. V. N. Golubkin and G. B. Sizykh, "Maximum principle for Bernoulli function," TsAGI Sci. J. **46**, 485–490 (2015).
13. E. Hopf, "Elementare Bemerkungen uber die Losungen partieller Differentialgleichungen zweiter Ordnung vom Elliptischen Typus," Sitzungsber. Preuss. Akad. Wissensch. **19**, 147–152 (1927).
14. C. Miranda, *Equazioni alle derivate parziali di tipo ellittico* (Springer, Berlin, Gottingen, Heidelberg, 1955).
15. A. I. Besportochnyy, A. N. Burmistrov, and G. B. Sizykh, "Variant of the Hopf theorem," Tr. MFTI **8** (1), 115–122 (2016).
16. V. V. Vyshinskiy, V. K. Ivanov, and A. V. Terpugov, "Simulation of complex flight regimes on aerobatic stands, taking into account atmospheric turbulence," Tr. MFTI **7** (1), 36–42 (2015).
17. V. V. Vyshinskii, "The program of generation of initial-boundary conditions in modeling the flow of landscape (WINDGUST)," State Registration Certificate of Computer Software No. 2015616444 (2015).
18. J. C. R. Hunt, A. A. Wray, and P. Moin, "Center for turbulence research," in *Proceedings of the Summer Program, 1988,* pp. 193–208.
19. J. Jeong and F. Hussain, "On the identification of a vortex," J. Fluid Mech. **285**, 69–94 (1995).
20. Y. Dubief and F. Delcayre, "On coherent-vortex identification in turbulence," J. Turbulence **1**, 1–22 (2000).
21. M. Lesieur, P. Begou, E. Briand, A. Danet, F. Delcayre, and J. L. Aider, "Coherent-vortex dynamics in large-eddy simulations of turbulence," J. Turbulence **4**, 1–16 (2003).
22. C. E. Cala, E. C. Fernandes, M. V. Heitor, and S. I. Shtork, "Coherent structures in unsteady swirling jet flow," Exp. Fluids **40**, 267–276 (2006).
23. I. S. Anufriev, Yu. A. Anikin, E. Yu. Shadrin, and O. V. Sharypov, "Diagnostics of swirl flow spatial structure in a vortex furnace model," Thermophys. Aeromech. **21**, 775–778 (2014).

Translated by L. P. Trubitsyna